LA-UR-02-5711

Approved for public release;
distribution is unlimited.

Title: MASS ABSORPTION CORRECTIONS FOR BETA COUNTING OF 147ND AND 147PM AND THE DETERMINATION OF K(147PM)/(K(147ND)

Author(s): Timothy Benjamin, C-INC
Scott Bowen, C-INC

Submitted to: AFTAC
September 2002

Los Alamos NATIONAL LABORATORY

Mass Absorption Corrections for β^- Counting of ^{147}Nd and ^{147}Pm and the Determination of K(^{147}Pm)/K(^{147}Nd)

Scott Bowen and Tim Benjamin

9/5/02

^{147}Nd is one of the primary fission products used in weapons radiochemical diagnostics to determine the fission efficiency of a nuclear test. Its 11-day half-life is very convenient for measurements of samples containing recently produced fission products. However, for samples more than approximately four months old, ^{147}Nd will have almost entirely died away. Fortunately, the beta-decay daughter of ^{147}Nd, ^{147}Pm, has a half-life of 2.6 years. Although ^{147}Nd can be readily gamma counted, a beta-decay based calibration has been maintained to ensure the best possible sensitivity on low-activity samples. A new calibration would add ^{147}Pm in order to extend the fission product measurements out to samples up to 25 years old.

^{147}Pm calibrations are complicated by several factors including: 1) poor gamma-counting rates, 2) beta-counting interference by ^{147}Nd during the first several months after a calibration irradiation, 3) lack of a stable Pm carrier for a radiochemically separated sample, and 4) the need for a mass absorption function for the relatively low endpoint beta energy (225KeV, average energy about 60KeV). All of these aspects can be overcome using data collected by S. Bowen as reported in a memo on 2/28/92 (see attachment 1).

Part I

^{147}Nd and ^{147}Pm Mass Absorption Corrections

The samples were prepared from aliquots of a stock solution consisting of the Nd fractions from several event 1152 'A' solutions with the addition of four different quantities of Nd carrier. The evolution of the parent-daughter, $^{147}Nd/^{147}Pm$, pair was followed for three to four months using Counter 25, shelf one, followed by another month of counting on Counter 14 in three different geometries. The principle difference between these two beta counters is the Compton-suppressed background of Counter 25. (Due to the high early count rates, it would have been better to use Counter 14 initially and then Counter 25 for the lower activity of the predominately ^{147}Pm daughter. Even better would have been to leave the samples on a single counter throughout.)

S. Bowen originally assessed the data with the codes 'CPM' and 'CLSQ' in his 1992 memo. The current evaluation uses a fully-weighted linear-least-squares code, 'Winfit', written by C. Duffy for the weapons radiochemistry program. The activity data from multi-component systems is linearized (see attachment 2). The background data for each sample is tested for outliers using Chauvenet's Criterion and the average value is applied to each measurement. The statistical uncertainties are compounded in the usual RMS (root-mean-square) manner and co-variances are included where necessary. In this instance, the slope of the regression line is a measure of the activity (cpm) of the ^{147}Nd at separation time (Table 1). The intercept contains information related to the ingrowth of the daughter ^{147}Pm as well as containing any ^{147}Pm that carried through the column separation. From these two values it is possible to calculate the relative counting efficiencies of these nuclides (Table 1). If the chemical separation is quantitative, then this efficiency ratio can be employed to characterize the relative count rate of the daughter ^{147}Pm in these samples.

Table 1

Sample	Counter	Shelf	20 mg Absorber	Mass (mg)	^{147}Nd cpm T_{sep}	sigma %	ε^{147}Pm/ε^{147}Nd	sigma %
5	25	1	No	5.284	1.394E+05	0.16%	0.208	0.86%
10	25	1	No	11.006	1.333E+05	0.10%	0.178	0.36%
15	25	1	No	16.211	1.280E+05	0.15%	0.161	1.0%
20	25	1	No	22.024	1.237E+05	0.12%	0.142	0.51%
10	14	1	No	11.006	1.292E+05	3.4%	0.178	4.2%
20	14	1	No	22.024	1.335E+05	4.1%	0.130	5.5%
5	14	2	No	5.284	8.248E+04	0.71%	0.224	0.98%
15	14	2	No	16.211	8.421E+04	0.59%	0.162	0.90%
5	14	2	Yes	5.284	4.790E+04	0.66%	0.0188	3.6%
15	14	2	Yes	16.211	4.921E+04	0.68%	0.0149	4.6%

The relative trends of ^{147}Nd cpm and ε^{147}Pm/ε^{147}Nd are consistent with expectations for the Counter 25 data. However, the ^{147}Nd cpm trends for the Counter 14 data is uniformly in the opposite direction. In all three geometries the heavier sample is higher by 2 to 3%. As these are the same samples as counted on Counter 25 and the efficiency ratios are all consistent with proper sample identification on Counter 14, a plausible cause of the count rate discrepancy is presented below in Part II. Only the Counter 25 data is used for the purpose of establishing ^{147}Nd and ^{147}Pm mass absorption curves.

Figure 1 contains the ^{147}Nd cpm data (with plotted 1σ uncertainties) vs. the weight of the sample (mg). Note that the error bars are of the same size as the plotted symbols. As the uncertainties are approximately equal, an unweighted Excel regression line is adequate. A quadratic function is used to model the expect curvature. This curvature is the result of the differential absorption of the two principle β^- decay energies of ^{147}Nd (15% at 370 KeV and 85% at 810 KeV). When this regression function is normalized to 15 mg (nominal 75% chemical yield on 20 mg of carrier) the mass absorption correction curve (Figure 2) results. Although the curvature of the quadratic in Figure 2 is small, it is the natural effect of the curvature shown in Figure 1.

Figure 1: ^{147}Nd Activity vs. Mass

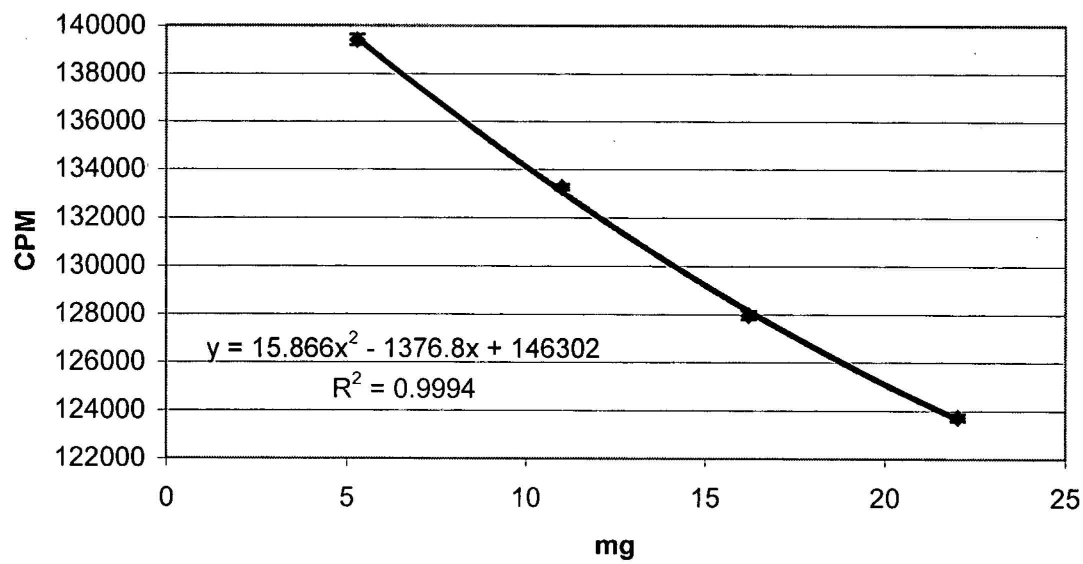

Figure 2: ^{147}Nd Correction wrt 15mg

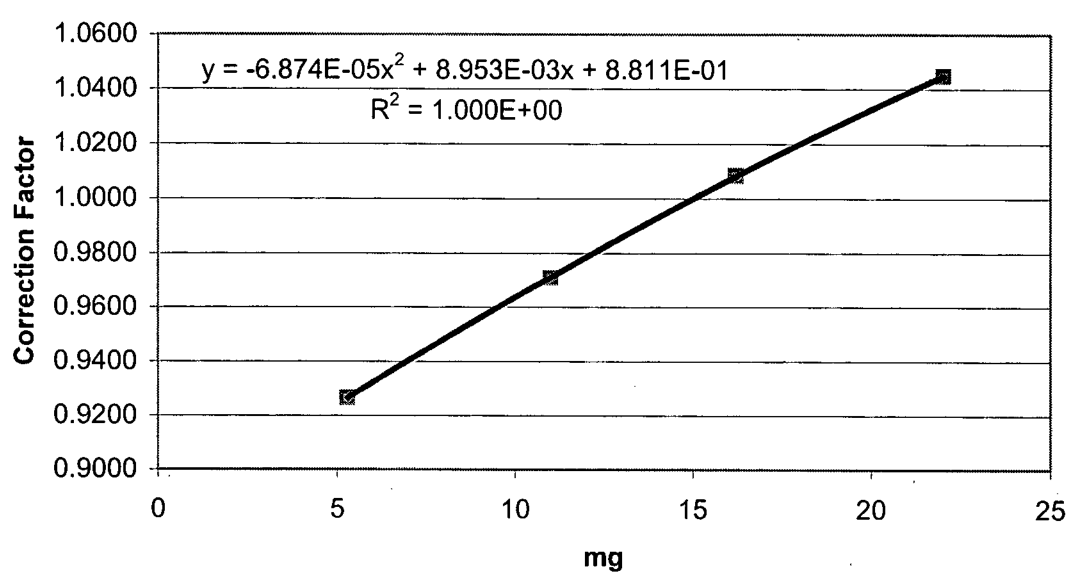

The calculated efficiency ratios as a function of mass are shown in Figure 3. These efficiency ratios were derived from the regressions of the counting data and are not a further application of the results shown in Figures 1 and 2. The error bars are again comparable to the size of the plotted symbols. The upper line is for the Counter 25 data, the lower line is for the Counter 14, Shelf 2, with the 20 mg absorber. The Counter 14 data for the geometries without the absorber are more uncertain and show some scatter but are consistent with the Counter 25 based line. Since incomplete separation of Pm from Nd would not be expected to be reproducible and therefore would introduce scatter into the efficiency ratio calculation, the tight array in Figure 3 is supportive of a clean separation. As expected, due to the different β^- energies of the two nuclides, slight curvature is observed in the data. The Counter 14 data with the absorber is underdetermined with respect to a quadratic fit; however, the absorber's suppression of both the ^{147}Pm and lower energy ^{147}Nd β^-'s would naturally result is less curvature than that observed for Counter 25 without the absorber.

Figure 3: ^{147}Pm/^{147}Nd Efficiency

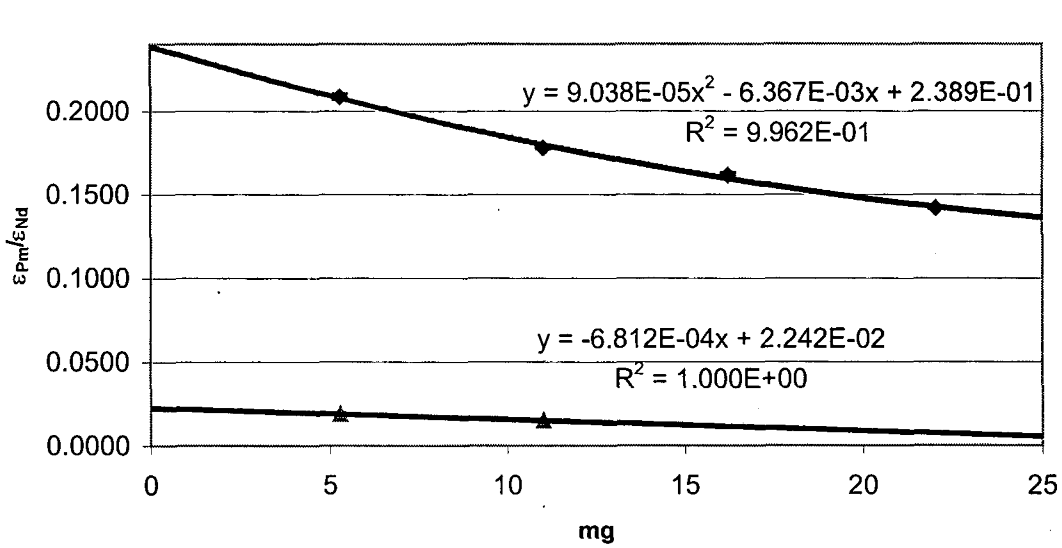

From the efficiency ratios and the deduced ^{147}Nd initial activities at separation time, the mass absorption curve for ^{147}Pm can be obtained. Multiplying the ^{147}Nd count rate by the ^{147}Pm/^{147}Nd efficiency ratio yields the relative ^{147}Pm count rate as a function of mass (Figure 4). In this instance, the curvature is due to the thicker samples beginning to approach infinite thickness for ^{147}Pm β^-'s. The shape of this curve should then be essentially 1/x. These results can then be used to construct the ^{147}Pm mass absorption curves (Figure 5) by simply normalizing to the nominal 15 mg value. As would be expected, the normalized data (the reciprocal of 1/x) show a linear correction. The low β^- energy results in a marked effect of nearly 3% per mg.

The final results are the two mass absorption correction functions for ^{147}Nd and ^{147}Pm. The uncertainties in the application of these correction factors is likely to be better than 1%, based on the quality of the data presented in these figures.

^{147}Nd correction factor = $0.8811 + 8.953\text{E-}3\ x_{mg} - 6.874\text{E-}5\ x_{mg}^{2}$

^{147}Pm correction factor = $0.5782 + 2.816\text{E-}2\ x_{mg}$

(Note that the ^{147}Nd correction presented by S. Bowen in 1992 averages only 0.4% higher than these presented here.)

Figure 4: ^{147}Pm Relative Activity vs. Mass

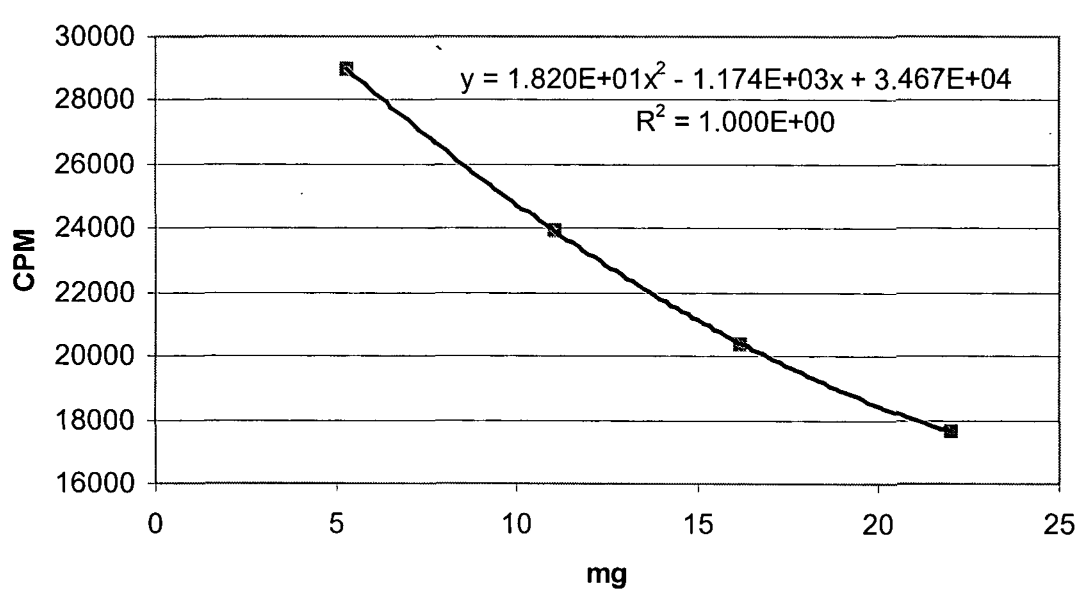

Figure 5: ^{147}Pm Correction wrt 15 mg

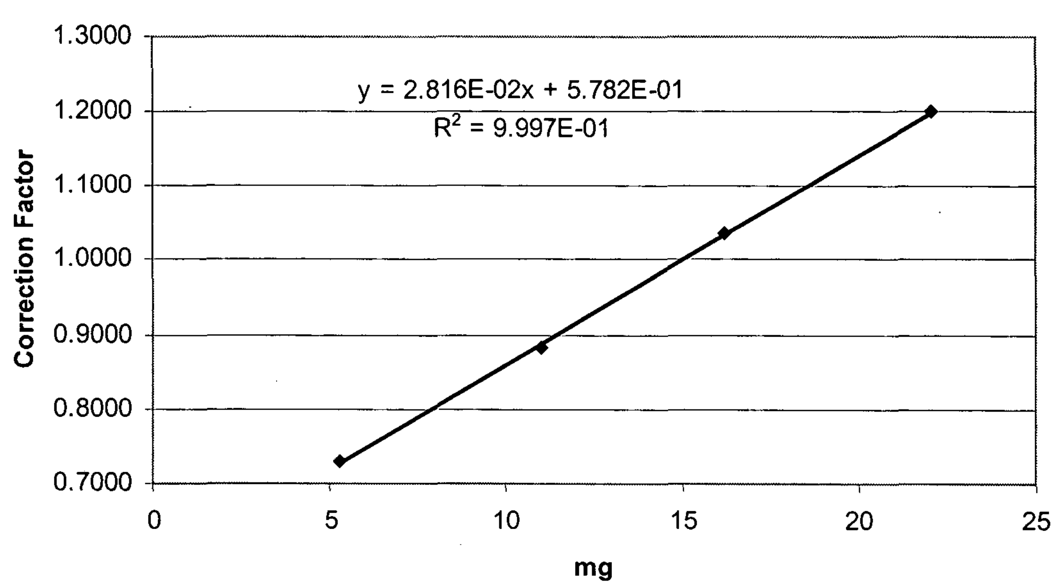

The ^{147}Pm/^{147}Nd K-Factor Ratio

The efficiency ratio relationship presented above can be used to calculate K-factor ratio for parent-daughter pairs like ^{147}Nd-^{147}Pm where the daughter's half-life is longer than the parent's. In this instance, the application would be converting the measured ^{147}Pm activity data to exactly the number of fissions that would have been measured at an earlier time by ^{147}Nd. Again, the uncertainties should be less than 1%.

$$K(^{147}Pm)/K(^{147}Nd) = \{(\lambda_{Nd} - \lambda_{Pm})/\lambda_{Pm}\}/\{\varepsilon_{Pm}/\varepsilon_{Nd})$$

For the 15 mg reference mass,

$K(^{147}Pm)/K(^{147}Nd) = 527$ (for Counter 25, Shelf 1, No Absorber)

$K(^{147}Pm)/K(^{147}Nd) = 7070$ (for Counter 14, Shelf 2, 20 mg/cm^2 Absorber)

Part II

The Apparent Counter 14 Anomaly

The observed increases in the calculated ^{147}Nd T_{sep} count rates for the heavier samples suggested a possible connection with the carrier itself (R. Gritzo, pers. comm.). The activity data from Table 1 is normalized to the corresponding Counter 25 data and presented in Table 2. (Note that the Counter 25 data is dominated by the actual decay of ^{147}Nd whereas the Counter 14 data is predominately ^{147}Pm daughter, which is used to calculate the equivalent ^{147}Nd parent, needed to support this activity.) Figure 6 is constructed from this Table. The linear fits indicate the relative efficiencies of the Counter 14 geometries. When the zero-mass (intercept) values are used to renormalized the data in Table 2, all the data is then on the same scale (intercept values becoming unity) (Figure 7). It is apparent that all three geometries show the same rate of increase with respect to carrier mass, 1.14% / mg.

Table 2

mg	Ctr14-1/Ctr25	Ctr14-2/Ctr25	Ctr14-2Abs/Ctr25
5.284		0.592	0.344
11.006	0.970		
16.211		0.658	0.385
22.024	1.079		

This is consistent with a model of a very minor contamination in the Nd carrier at this time. Based on the last counts of the samples on Counter 14, shelf 2, with absorber, the apparent contaminant amounts to 0.20 cpm/mg. From the Figure 6 relative efficiencies, the count rate for the other two geometries would be 0.35 cpm/mg (Counter 14, shelf 2, without absorber) and 0.53 cpm/mg (Counter 14, shelf 1, without absorber). These count rates are too small to affect the high-activity ^{147}Nd results from Counter 25. These data demonstrated that low count rate samples are sensitive to very small sources of contamination.

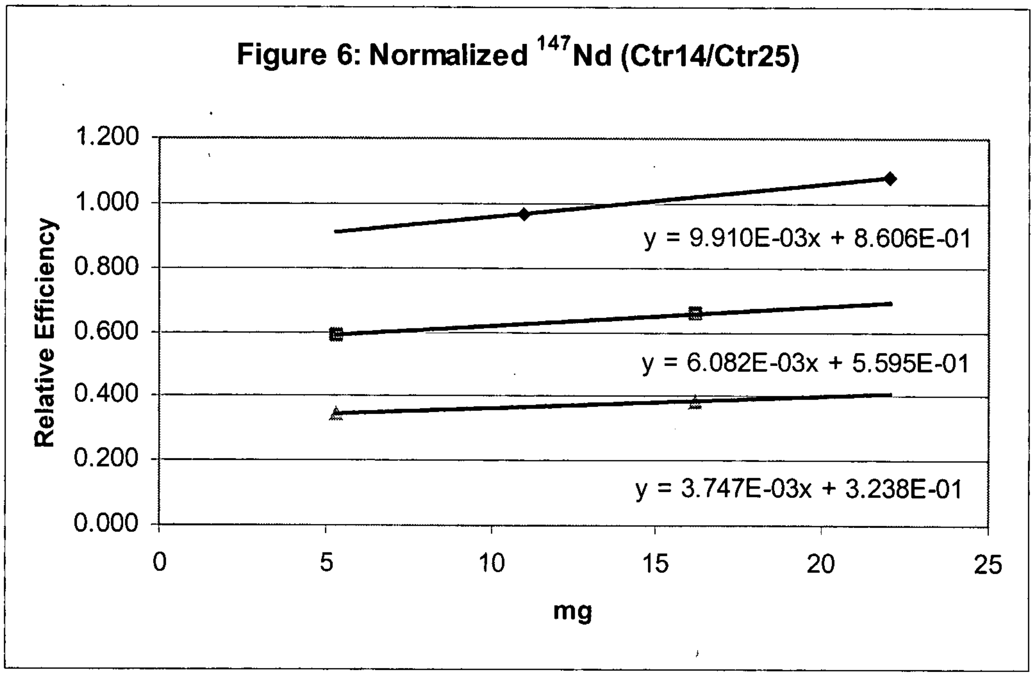

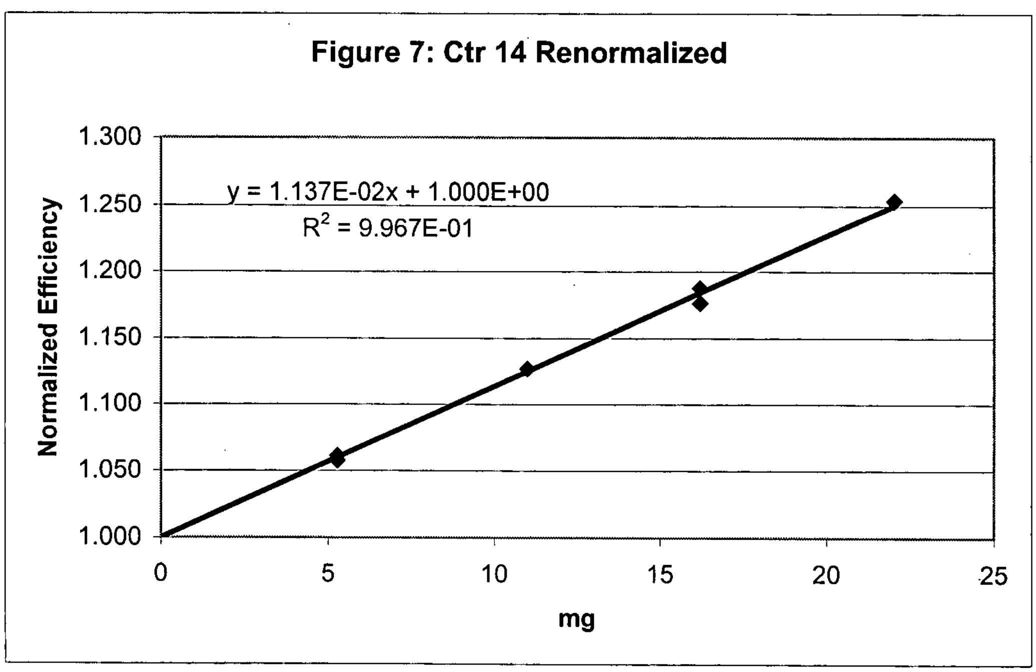

Promethium-147 Experiment

02/28/92

1) The following tube numbers from the Ln HPLC run on shot 1152 were combined in a 50 mL Erlenmeyer flask:

Jug Number	Tubes
2	195-205
3	194-204
4	196-205
5	195-204
6	197-204

2) The sample was boiled to dryness and heated at 600 °C for approximately one hour.

3) The sample was dissolved in concentrated HCl, a mixture of HNO_3 and $HCLO_4$ was added, and the sample was fumed to near dryness.

4) The sample was transferred to a 500 mL volumetric flask with 3M HCl and the volume brought up to 500 mL with 3 M HCl. This was the stock solution.

5) 1, 3, and 5 mL fractions of the stock were removed and placed in plastic scintillation vials. All volumes were brought up to 5 mL with H_2O and counted on Ge(Li) counter 76, shelf 10. RAYGUN analysis of the three samples for ^{147}Nd atoms at 308.542,1991 (the estimated Nd-Pm separation time for the columns) per mL of solution gave values of 9.125E9 ± 0.6%, 9.190E9 ± 0.5%, and 9.212E9 ± 0.6%, respectively.

6) Four 1 mL fractions of the stock solution were removed and placed in centrifuge cones with 0.5, 1.0, 1.5, and 2.0 mL of standardized Nd carrier (11.42 mg Nd_2O_3 per mL). The oxides were precipitated with NH_4OH, fired at 1100 °C

for 30 minutes, weighed, and mounted on Al counting cards in the standard lanthanide oxide mounting geometry.

ML added	Ppt weight	Chem yield
0.5	5.284 mg	0.9254
1.0	11.006 mg	0.9638
1.5	16.211 mg	0.9464
2.0	22.024 mg	0.9643

7) The mounted samples were first counted on Ge(Li) counter 72, shelf 10 to measure ^{147}Nd atoms at 308.542,1991. This gave the following results:

Ppt weight	Atoms at T/mL
5.284 mg	9.073E9±0.64%
11.006 mg	9.326E9±0.82%
16.211 mg	9.164E9±0.70%
22.024 mg	9.324E9±0.61%

8) The samples were next counted on beta counter 25, shelf 1 (no absorber). The CPM program was run on the data from these samples using 2 components (^{147}Pm, $t_{1/2}$ = 2.623 years and ^{147}Nd, $t_{1/2}$ = 10.990 days). The CLSQ program was also run. The following ^{147}Nd values were obtained:

Weight (mg)	Cpm at T (CPM)	Err %	Cpm at T (CLSQ)	Err %
5.284	1.377E5	0.1	1.377E5	1.5
11.006	1.315E5	0.1	1.314E5	1.0
16.211	1.264E5	0.1	1.262E5	1.5
22.024	1.221E5	0.1	1.219E5	0.9

These values are plotted on the attached plot. The y-intercept, 1.422E5, is the extrapolated no mass absorption cpm value. A plot of measured cpm divided by 1.422E5 versus sample mass gives a mass absorption correction curve. This is also attached.

The corresponding ^{147}Pm values obtained from these beta analyses were:

Weight (mg)	Cpm at T (CPM)	Err %	Cpm at T (CLSQ)	Err %
5.284	3.302E2	0.7	3.296E2	4.8
11.006	2.709E2	0.3	2.682E2	1.6
16.211	2.339E2	0.9	2.348E2	6.1
22.024	2.012E2	0.3	2.015E2	1.8

These samples were also counted on beta counter 14 with some of the samples counted through a 20 mg absorber to reduce the ^{147}Pm beta contribution. The data for counts with the absorber present were analyzed by assuming either a one or two component system.

The Nd results were:

Weight (mg)	Absorber	Cpm at T (CPM)	Err %	Cpm at T (CLSQ)	Err %
5.284	No	8.177E4	0.6	8.126E4	2.0
5.284	Yes	5.389E4	0.8	5.798E4	0.4
5.284*	Yes	4.492E4	3.0	4.759E4	0.8
11.006	No	1.266E5	5.0	1.445E5	12.8
16.211	No	8.291E4	0.6	8.302E4	1.6
16.211	Yes	5.794E4	0.9	5.713E4	0.4
16.211*	Yes	4.995E4	1.3	4.897E4	0.8
22.024	No	1.296E5	5.6	1.463E5	10.1

* Two component calculation

The Pm results were:

Weight (mg)	Absorber	Cpm at T (CPM)	Err %	Cpm at T (CLSQ)	Err %
5.284	No	2.112E2	0.3	2.115E2	0.8
5.284	Yes	-	-	-	-

Attachment 1

5.284*	Yes	1.388E1	14.9	9.785	3.1
11.006	No	2.640E2	1.2	2.564E2	3.7
16.211	No	1.560E2	0.4	1.561E2	0.8
16.211	Yes	-	-	-	-
16.211*	Yes	7.184	7.5	7.774	3.8
22.024	No	1.949E2	1.9	1.877E2	4.0

* Two component calculation

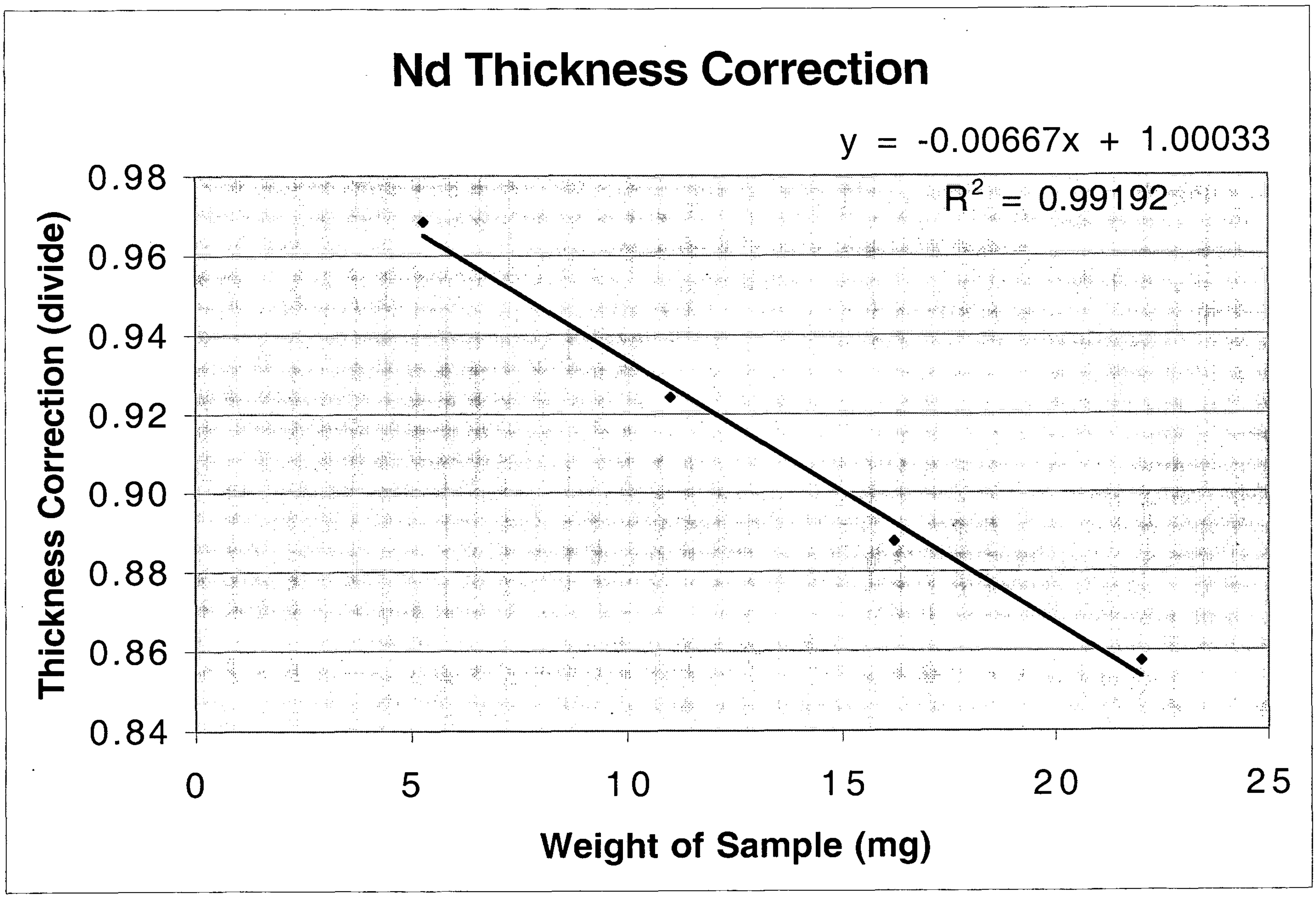
Nd Thickness Correction
y = -0.00667x + 1.00033
R2 = 0.99192
Thickness Correction (divide)
0.98
0.96
0.94
0.92
0.90
0.88
0.86
0.84
0
5
10
15
20
25
Weight of Sample (mg)

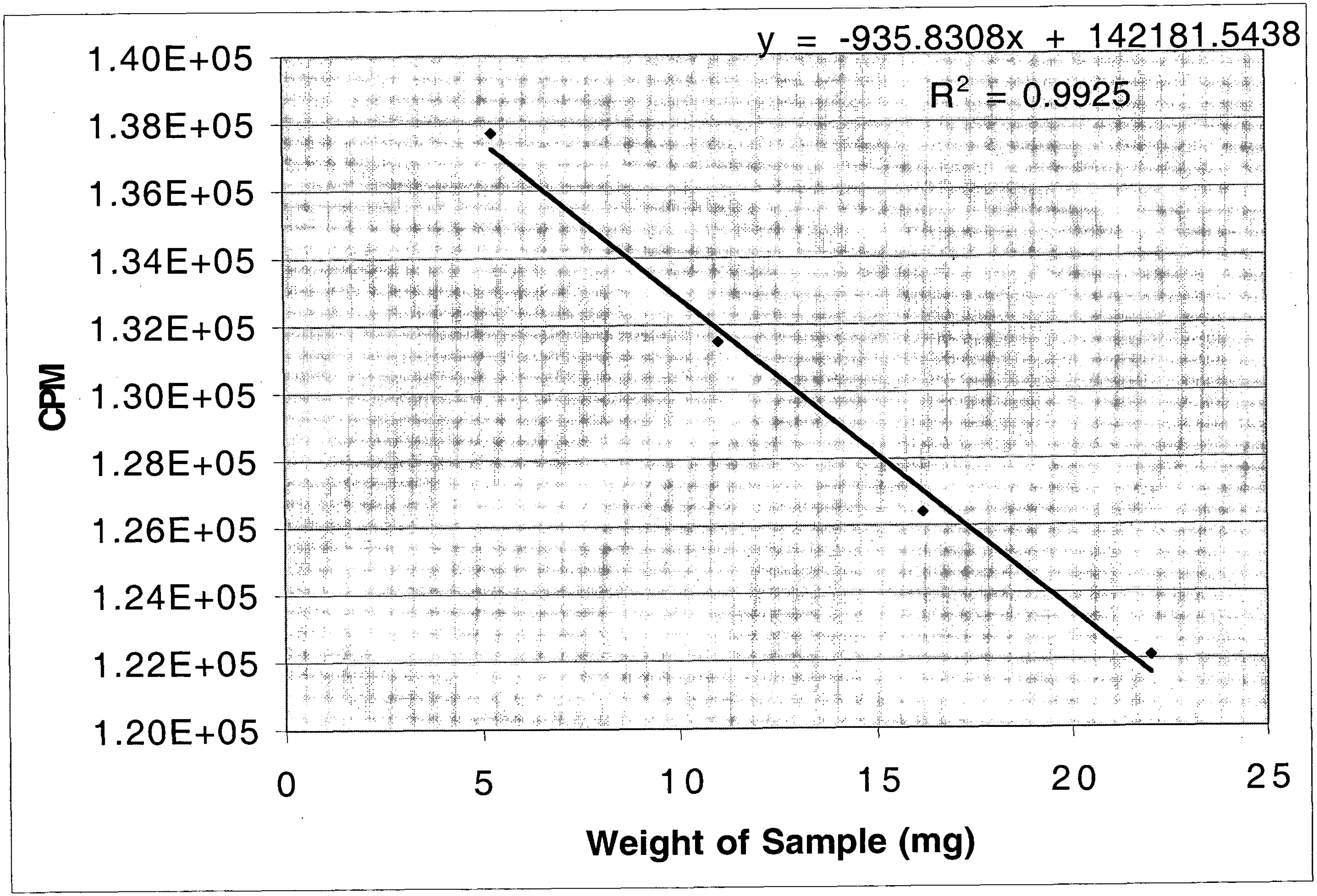

y = -935.8308x + 142181.5438
R^2 = 0.9925
1.40E+05
1.38E+05
1.36E+05
1.34E+05
1.32E+05
1.30E+05
1.28E+05
1.26E+05
1.24E+05
1.22E+05
1.20E+05
CPM
0
5
10
15
20
25
Weight of Sample (mg)

Attachment 2

Math Я Us

Parent(1)-Daughter(2) Equilibrium:

Total Activity / Parent Activity

1) $= [\lambda_1 n_1^o\{\varepsilon_1 e^{-\lambda 1\Delta t} + (\lambda_2\varepsilon_2/(\lambda_2-\lambda_1))(e^{-\lambda 1\Delta t} - e^{-\lambda 2\Delta t})\} + \lambda_2 n_2^o\varepsilon_2 e^{-\lambda 2\Delta t}] / \lambda_1 n_1^o\varepsilon_1 e^{-\lambda 1\Delta t}$

2) $= e^{(\lambda 1\Delta t)}\{e^{-\lambda 1\Delta t} + (\varepsilon_2/\varepsilon_1)(\lambda_2/(\lambda_2-\lambda_1))(e^{-\lambda 1\Delta t} - e^{-\lambda 2\Delta t}) + (\lambda_2 n_2^o\varepsilon_2/\lambda_1 n_1^o\varepsilon_1)e^{-\lambda 2\Delta t}\}$

3) $= 1 + (\varepsilon_2/\varepsilon_1)(\lambda_2/(\lambda_2-\lambda_1))(1- e^{(\lambda 1-\lambda 2)\Delta t}) + (\lambda_2 n_2^o\varepsilon_2/\lambda_1 n_1^o\varepsilon_1)e^{(\lambda 1-\lambda 2)\Delta t}\}$

For $\lambda_2 > \lambda_1$ and at $t \rightarrow \infty$ (equilibrium)

4) $= 1 + (\varepsilon_2/\varepsilon_1)(\lambda_2/(\lambda_2-\lambda_1))$

Linear Regression of Parent(1)-Daughter(2) Activity Curve:

Total (measured) Activity (for a perfect separation, $n_2^o = 0$)

5) Total $= \lambda_1 n_1^o\{\varepsilon_1 e^{-\lambda 1\Delta t} + (\lambda_2\varepsilon_2/(\lambda_2-\lambda_1))(e^{-\lambda 1\Delta t} - e^{-\lambda 2\Delta t})\} + \lambda_2 n_2^o\varepsilon_2 e^{-\lambda 2\Delta t}$

Linearization

6) Total $(e^{\lambda 2\Delta t}) = \lambda_1 n_1^o\varepsilon_1\{e^{(\lambda 2-\lambda 1)\Delta t} + (\varepsilon_2/\varepsilon_1)(\lambda_2/(\lambda_2-\lambda_1))(e^{(\lambda 2-\lambda 1)\Delta t} - 1)\} + \lambda_2 n_2^o\varepsilon_2$

where the slope is $\lambda_1 n_1^o\varepsilon_1$ and the intercept is $\lambda_2 n_2^o\varepsilon_2$; and at equilibrium,

7) $\text{Total}^o = \{1 + (\varepsilon_2/\varepsilon_1)(\lambda_2/(\lambda_2-\lambda_1))\}\lambda_1 n_1^o\varepsilon_1$

but a priori $(\varepsilon_2/\varepsilon_1)$ is both a function of sample mass and is assumed to be unknown, therefore, define and effective efficiency for the counting, ε^*, so that,

8) $\text{Total}^o = \{1 + (\lambda_2/(\lambda_2-\lambda_1))\}\lambda_1 n_1^o\varepsilon^*$

and,

9) $\{1 + (\lambda_2/(\lambda_2-\lambda_1))\}\lambda_1 n_1^o\varepsilon^* = \{1 + (\varepsilon_2/\varepsilon_1)(\lambda_2/(\lambda_2-\lambda_1))\}\lambda_1 n_1^o\varepsilon_1$

10) $\varepsilon^* = \varepsilon_1\{1 + (\varepsilon_2/\varepsilon_1)(\lambda_2/(\lambda_2-\lambda_1))\} / \{1 + (\lambda_2/(\lambda_2-\lambda_1))\}$

11) Slope $= \lambda_1 n_1^o\varepsilon^*$

12) Intercept $= \lambda_2 n_2^o\varepsilon_2 + \lambda_1 n_1^o(\varepsilon_1 - \varepsilon_2)(\lambda_2/(2\lambda_2-\lambda_1))$

Apply $K_T(\varepsilon^*)$ or $K_1(\varepsilon^*)$ to eqn 8 or eqn 11.